

# UNIVERSITI SAINS MALAYSIA



UNIVERSITI SAINS MALAYSIA

**Effect of Physical Filters (Aluminum 0.2mm  
and 0.3mm thick) on Sensitivity, Uniformity,  
and Spatial Resolution of Toshiba GCA-  
901A/HG Gamma Camera with Tc-99m in  
Planar Imaging**

Dissertation submitted in partial fulfillment for  
the award of the  
Bachelor's Degree of Health Science in Medical  
Radiation

**Siti Nazipah Binti Mohamad Nawi**

School of Health Sciences  
Universiti Sains Malaysia  
Health Campus  
16150, Kubang Kerian, Kelantan  
Malaysia

2004

# UNIVERSITI SAINS MALAYSIA



UNIVERSITI SAINS MALAYSIA

**Effect of Physical Filters (Aluminum 0.2mm  
and 0.3mm thick) on Sensitivity, Uniformity,  
and Spatial Resolution of Toshiba GCA-  
901A/HG Gamma Camera with Tc-99m in  
Planar Imaging**

Dissertation submitted in partial fulfillment for  
the award of the  
Bachelor's Degree of Health Science in Medical  
Radiation

**Siti Nazipah Binti Mohamad Nawi**

School of Health Sciences  
Universiti Sains Malaysia  
Health Campus  
16150, Kubang Kerian, Kelantan  
Malaysia

2004

## CERTIFICATE

This is to certify that the dissertation entitled  
“Effect of physical filters (Aluminum 0.2 mm and 0.3 mm thick) on sensitivity, uniformity,  
and spatial resolution of Toshiba GCA-901A/HG gamma camera with Tc-99m in planar  
imaging”

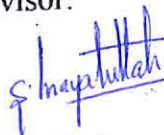
is the bonafide record of research work done by

Ms SITI NAZIPAH MOHAMAD NAWI

during the period from January to March 2004

under my supervision.

Signature of Supervisor:



Dr. Sayed Inayatullah Shah

School of Health Sciences  
Universiti Sains Malaysia  
16150 Kubang Kerian Kelantan  
Malaysia

28 April 2004

## CERTIFICATE

This is to certify that the dissertation entitled

“Effect of physical filters (Aluminum 0.2 mm and 0.3 mm thick) on sensitivity, uniformity, and spatial resolution of Toshiba GCA-901A/HG gamma camera with Tc-99m in planar imaging”

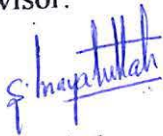
is the bonafide record of research work done by

Ms SITI NAZIPAH MOHAMAD NAWI

during the period from January to March 2004

under my supervision.

Signature of Supervisor:



Dr. Sayed Inayatullah Shah

School of Health Sciences  
Universiti Sains Malaysia  
16150 Kubang Kerian Kelantan  
Malaysia

28 April 2004

## **ACKNOWLEDGEMENT**

The preparation of this research project has been aided by the significant contributions of many individuals, which are gratefully acknowledged. I wish to express my sincere appreciation to Dr Sayed Inayatullah Shah, as my supervisor for encouragement and support in this research. I appreciate the support and guidance of Associate Prof Ahmad Zakaria, chairman of Medical Radiation course, for my research project. I also wish to express my appreciation to En Waidi Abdullah and also En Ismail who have provided much advice and technical support to finish my research project. Lastly, I would like to thank to Department of Nuclear Medicine, Radiotherapy, and Oncology for allowing me to use the equipment.

## TABLE OF CONTENTS

	Page
<b>Title</b>	<b>i</b>
<b>Certificate</b>	<b>ii</b>
<b>Acknowledgement</b>	<b>iii</b>
<b>Table of Contents</b>	<b>iv</b>
<b>List of tables, figures, and graphs</b>	<b>v</b>
<b>Abstract</b>	<b>1</b>
<b>Introduction</b>	<b>2</b>
<b>Review of literature</b>	<b>4</b>
<b>Objectives of the study</b>	<b>6</b>
<b>Materials and methods</b>	<b>7</b>
<b>Results</b>	<b>14</b>
<b>Sensitivity analysis</b>	<b>14</b>
<b>System spatial resolution analysis</b>	<b>15</b>
<b>Field uniformity analysis</b>	<b>22</b>
<b>Discussion</b>	<b>24</b>
<b>Sensitivity analysis</b>	<b>24</b>
<b>System spatial resolution</b>	<b>25</b>
<b>Field uniformity</b>	<b>26</b>
<b>Conclusion</b>	<b>27</b>
<b>References</b>	<b>28</b>

## LIST OF TABLES, FIGURES, AND GRAPHS

	<b>Page</b>
<b>Figure 1:</b> Toshiba GCA 901/HG gamma camera	7
<b>Figure 2:</b> Collimators	8
<b>Figure 3:</b> Flood field phantom	9
<b>Figure 4:</b> Aluminum filter	10
<b>Figure 5:</b> Technetium-99m	10
<b>Figure 6:</b> System sensitivity setup	11
<b>Figure 7:</b> Line source	12
<b>Figure 8:</b> Spatial resolution setup	12
<b>Figure 9:</b> Field uniformity setup	13
<b>Table 1:</b> The sensitivity without and with material filters for LEHR collimator	14
<b>Table 2:</b> The sensitivity without and with material filters for LEGP collimator	15
<b>Graph 1:</b> The FWHM values in air and scattering medium without and with aluminum 0.2 mm filter with LEHR collimator	16
<b>Graph 2:</b> The FWHM values in air and scattering medium without and with aluminum 0.3 mm filter with LEHR collimator	16
<b>Graph 3:</b> The FWHM values in air and scattering medium without and with aluminum 0.2 mm and 0.3 mm filter with LEHR collimator	17
<b>Graph 4:</b> The FWTM values in air and scattering medium without and with aluminum 0.2 mm filter with LEHR collimator	17
<b>Graph 5:</b> The FWTM values in air and scattering medium without and with aluminum 0.3 mm filter with LEHR collimator	18

<b>Graph 6:</b> The FWTM values in air and scattering medium without and with aluminum 0.2 mm and 0.3 mm filter with LEHR collimator	<b>18</b>
<b>Graph 7:</b> The FWHM values in air and scattering medium without and with aluminum 0.2 mm filter with LEGP collimator	<b>19</b>
<b>Graph 8:</b> The FWHM values in air and scattering medium without and with aluminum 0.3 mm filter with LEGP collimator	<b>19</b>
<b>Graph 9:</b> The FWHM values in air and scattering medium without and with aluminum 0.2 mm and 0.3 mm filter with LEGP collimator	<b>20</b>
<b>Graph10:</b> The FWTM values in air and scattering medium without and with aluminum 0.2 mm filter with LEGP collimator	<b>20</b>
<b>Graph11:</b> The FWTM values in air and scattering medium without and with aluminum 0.3 mm filter with LEGP collimator	<b>21</b>
<b>Graph 12:</b> The FWTM values in air and scattering medium without and with aluminum 0.2 mm and 0.3 mm filter with LEGP collimator	<b>21</b>
<b>Table 3:</b> The UFOV and CFOV uniformity shown in integral and differential uniformity without and with material filters with LEHR collimator	<b>23</b>
<b>Table 4:</b> The UFOV and CFOV uniformity shown in integral and differential uniformity without and with material filters with LEGP collimator	<b>24</b>
<b>Figure10:</b> The uniformity without material filter with LEHR collimator	<b>24</b>
<b>Figure 11:</b> The uniformity with aluminum 0.2 mm thick with LEHR collimator	<b>25</b>
<b>Figure 12:</b> The uniformity with aluminum 0.3 mm thick with LEHR collimator	<b>25</b>
<b>Figure 13:</b> The uniformity without material filter with LEGP collimator	<b>26</b>
<b>Figure 14:</b> The uniformity with aluminum 0.2 mm thick LEGP collimator	<b>26</b>
<b>Figure 15:</b> The uniformity with aluminum 0.3 mm thick LEGP collimator	<b>27</b>

## **ABSTRACT**

The performance of a scintillation-camera system is assessed to assure the acquisition of diagnostically reliable images. Decisions-making data to determine acceptability of camera performance are acquired when some parameters are tested. So, in this study the sensitivity, uniformity and system spatial resolution parameters are tested by using physical filters, aluminum 0.2 mm and aluminum 0.3 mm. The Tc-99m is used as a source. Two collimator are used which are low energy parallel-hole collimators, i.e. low energy high resolution (L.E.H.R.) and low energy general purpose (L.E.G.P.). The reason for this choice was that these collimators are the most commonly used for clinical studies in nuclear medicine departments. For data acquisition, the method utilizes a photopeak energy window ranging 126 keV-154 keV of Tc-99m spectrum with 128 x 128 matrix size were used for all tests. From sensitivity, uniformity, and spatial resolution results material filtered data shows an improvement.

## INTRODUCTION

The performance of a scintillation-camera system must be assessed to assure the acquisition of diagnostically reliable images [8]. Performance can be affected by changes or failure of individual system components or subsystems and environmental conditions. Decision-making data to determine acceptability of camera performance can be acquired when the parameters of field uniformity, spatial resolution, linearity, and sensitivity are tested.

Planar imaging is two-dimensional portrayal of three-dimensional or four-dimensional distribution [6]. Planar acquisition of data is also the basis of many types of tomographic imaging. A planar imaging system requires the information of the direction in which the photon was traveling upon striking the crystal detector, the location of its interaction with the detector, and the energy of the photon [6]. The direction of travel and point of interaction define a line somewhere along which the photon must have been emitted. Photon energy is used to discriminate those photons that have scattered between their site of emission and detection and those that have not.

In nuclear medicine, the intermixing of primary, scattered, and other kinds of radiation in scintillation detector's energy spectrum causes a troublesome background in planar images [3]. Most of the photons reaching the detector have traveled from the patient along paths parallel to the collimator's holes, or nearly so. These include the primary gamma ray, which are strongly correlated with the location of the nuclide that decayed. The detector also registers event due to other processes, for example, septum-penetration gamma rays and

fluorescence x-ray originating in the lead collimator. The challenge has long been to make the best possible use of this mixture of primary and background radiation.

System spatial resolution is one of the common performance parameters for gamma cameras [7]. It has been defined as the ability of imaging system to distinguish two closely spaced objects and is a fundamental parameter for comparing systems. The simplest method of examining system spatial resolution is to determine the full half maximum (FWHM) and full width at tenth maximum (FWTM) in the image of line source (the line spread function, LSF).

System sensitivity parameter closely relate to spatial resolution of radionuclide imaging units parameter. Poor sensitivity can only produce noisy, low resolution images [4].

Flood field uniformity is done to check the uniformity of the camera response to a uniform irradiation of the detector [6].

All the tests should be done carefully especially technical procedure to avoid re-take data acquisition.

## REVIEW OF LITERATURE

The use of scintillation detector gamma cameras in single photon emission imaging, particularly for dynamic radionuclide studies, frequently results in count rates which are high enough to produce pulse pile-up and cause data losses due to high dead time. Previously, gamma camera systems were able to handle less count rate. A small fraction of all detected counts are accepted, the remainder, resulting from scattered radiation characteristic x-rays of lead (Pb), being rejected by a pulse height analyzer (PHA), most of the observation time is wasted in analyzing and eliminating pulses [Muehllehner et al 1974]. In 1975, Muehllehner applied the technique to positron emission tomography (PET) by employing a filter which consisted of 1.27 mm of lead, 0.76 mm of tin and 0.25 mm of copper. With that filter, a factor of five increase in useful count rate was reported. Then, Ficke and Ter-Pogossian [1990], suggested that material filters might be advantageous in reducing low energy radiation originating in the field of view of the scanner. They analysed the spectrum from NaI(Tl) detectors by using 0.43 mm and 0.86 mm thick lead (Pb) filters in PET. As a result of applying these filters low energy events were reduced by some 30 – 40 % for the loss of 7 – 12 % photopeak (unscattered) events.

Harshaw Scintillation Phosphors (1975) has indicated that it could be possible to design an appropriate absorbing filter by combining various detector materials. Then, Strand and Larsson (1978) published a paper in which they suggested that it may be possible to reduce the recording of undesirable (scattered) photons by means of specially made attenuating filters.

In 1986, Pillay and his colleagues applied an alloy filter, consisting of Pb, Zn, and Sn, in single planar imaging. From various patient studies they claimed improvement in the quality (contrast) of images.

Later, according to Shah SI (1993), material filtered data shows an improvement in all tested parameters of spatial resolution, modulation transfer function, single slice sensitivity and numerical analysis of a uniformity filled TC-99m cylindrical phantom's reconstructed image of Tc-99m spectrum in conjunction with material filter. The tests were done with GE 400 XC/T gamma camera. Whereas this project were done to study the effects of physical filters (Al 0.2 mm and 0.3 mm thick) on sensitivity, uniformity and system spatial resolution of Toshiba GCA-901A gamma camera with Tc-99m in planar imaging. This method utilizes a photopeak energy window ranging (126-154 keV) 20% centered at 140 keV.

## **OBJECTIVES OF THE STUDY**

- to study the effects of physical filters on sensitivity, uniformity and system spatial resolution of Toshiba GCA-901A gamma camera with Tc-99m in planar imaging.
- to compare the results obtained from the data acquired by employing physical filter with those data obtained by using no filter.

## MATERIALS AND METHODS

A gamma camera converts photons emitted by the radionuclide in the patient into a light pulse and subsequently into a voltage signal. This signal is used to form an image of the distribution of the radionuclide. Gamma camera may be classified as either analog or digital types. Most of the newer cameras incorporate digital features and the gamma camera that is used in this research is a digital type [6]. The main advantages of digital cameras are much faster, can interact directly with the computer, and generally require less maintenance.

Gamma camera that was used in this research is Toshiba GCA 901A/HG. The most important of any gamma camera computer system is the software. The gamma camera is interfaced with the software GMS-5500 that is shared by the medical image processing between the instruments.



Figure 1: Toshiba GCA 901/HG gamma camera

To form the image of an object with a gamma camera, it is required to project gamma-photons from the radioactivity distribution onto the scintillation detector of scanning system [4]. For planar imaging, collimators are mounted on the face of the detector of the

gamma camera and are interchangeable depending on the type of study and the energy of the radionuclide to be used. A collimator allows only those gamma-photons traveling in a specified direction. This procedure inevitably results in a significant decrease in the number of detected gamma photons, resulting in reduced sensitivity, or increased acquisition time. The precise collimation of the gamma-photons is necessary not only to obtain accurate spatial distribution of the gamma-photon emitting radionuclide, but also to eliminate at least some of the scattered gammas which would impair contrast.

Two collimators were used which are low energy parallel-hole collimators are employed, low energy high resolution (L.E.H.R.) and low energy general purpose (L.E.G.P.). The reason for this choice was that these collimators are the most commonly used for clinical studies. Besides, low energy collimators generally refer to a maximum energy of 150 keV, whereas medium-energy collimators have a maximum suggested energy of about 400 keV[7].



Figure 2: Collimators

The flood phantom provides a convenient means of lighting a scintillation camera's crystal to determine response uniformity over the entire field, and the ability to be used as a transmission source on organ imaging [10]. The model that used in this research was

rectangular flood phantom model #043-050 from Atomic Products Corporation and the specification of this flood phantom are :

Dimension: 48.3cm x 63.5cm x 3.2cm

Cavity : 38.1cm x 53.3cm x 1.3cm



Figure 3: Flood field phantom

To reduce the effects of scattered radiation, particularly in low-count images, smoothing of the image can be performed. Smoothing is accomplished through the use of digital filters [7]. Aluminum filter was chosen with two thicknesses which are 0.2 mm and 0.3 mm thick to compare the results obtained from the two different filters thickness. The filters are rectangular shaped with 57 cm x 42 cm.



Figure 4: Aluminum filter

The radionuclides used for evaluation of most gamma camera systems are Tc-99m and Co-57 [7]. Technetium 99m has the advantage of being low cost which is used in most of the clinical imaging procedures.



Figure 5: Technetium-99m

### **Data acquisition for system sensitivity, spatial resolution, and uniformity measurements without and with a material filter**

For planar imaging, when more counts are collected, an image of improved quality (less noise) is obtained [4]. The sensitivity and spatial resolution of radionuclide imaging units are two closely related parameters. The sensitivity depends upon the total solid angle subtended by the detector at the source [4]. If this solid angle is made as large as possible, then the spatial resolution is likely to be poor. In system sensitivity measurement, the source, 3.43 mCi of Tc-99m was filled into 1/3 of Petri dish. Then the Petri dish was placed on the collimator, and data were gathered without and with material filter.

For this study, the 1 000 000 counts collected in the image matrix 128 x 128 resolution for both LEHR and LEGP collimator. Before that, background counts were measured for accurate results. For relevant measurements, the filter was mounted on the outer side of collimator and the acquisition parameters were the same as those without filter.



Figure 6: System sensitivity test setup

To obtain system spatial resolution data, a line source filled with 1.877 mCi Tc-99m solution of internal diameter 2.0 mm and 30.0 cm in length for LEHR collimator and 16.364 mCi for LEGP collimator was scanned at various distances from the surface of the gamma

camera collimator. The gamma camera Toshiba GCA 901 A/HG was used. Planar images using acrylic plate which is water equivalent scattering medium at different depths were obtained without and with material filter. The dimension of the acrylic equivalent water plates is 30 cm x 30 cm. These were varied according to the required thickness of the scattering medium. The increment of distance is 1 cm until the distance reached to 10 cm from the source. Data were collected by employing a material filter either with a LEGP and, or with LEHR collimator with 20% photopeak energy window centered at 140keV. The mode of acquisition was a 128 x 128 x 1 matrix for both collimators. The total counts in the photopeak window per emission image (without and with material filter) was maintained at 1 000 000 counts for LEHR collimator and 2 500 000 counts for LEGP collimator.



Figure 7: Line source



Figure 8: Spatial resolution test setup

The field uniformity data were obtained with flood phantom described on page 34. The phantom was filled to ninety-five percent (95%) capacity with water that will solubilize the radioactive material to be added [10]. Activity 14.19 mCi of Tc-99m was added into the phantom. The phantom was sealed with the thumb screws previously removed. The phantom was rotated in such a manner as to allow the air space remaining to move through the phantom. It was left for two hours to insure a homogenous mixture. Images were collected by employing a material filter with either a LEGP or LEHR collimator. The photopeak energy window 20% centered at 140 keV was selected. The mode of acquisition was a 128 x 128 x 1 matrix for both collimators. The total counts in the photopeak window per emission image (without and with material filter) was maintained at 20 000 000 counts.



Figure 9: Field uniformity test setup

## RESULTS

### Sensitivity analysis

The sensitivity and spatial resolution of radionuclide imaging units are two closely related parameters. The sensitivity depends up on the total solid angle subtended by the detector at the source [4]. The sensitivity is the ratio of counts observed divided by nuclear disintegrations. It can be determine by the equation of

$$\text{Sensitivity} = \frac{\text{counts per second (cps)}}{\text{Activity of radionuclide (mCi)}} \quad [8]$$

The greater the fraction of the emitted photons that are detected, the higher the sensitivity. There is a “trade-off” between resolution and sensitivity with respect to the photon energy and the thickness of lead septa required in collimators designed for use with higher-energy photons. The results were described into table (1) and table (2).

Sensitivity (cps/mCi)	
No Filter	4028.40
Al 0.2mm	4011.03
Al 0.3mm	3991.45

Table 1: The sensitivity without and with material filter for LEHR collimator.

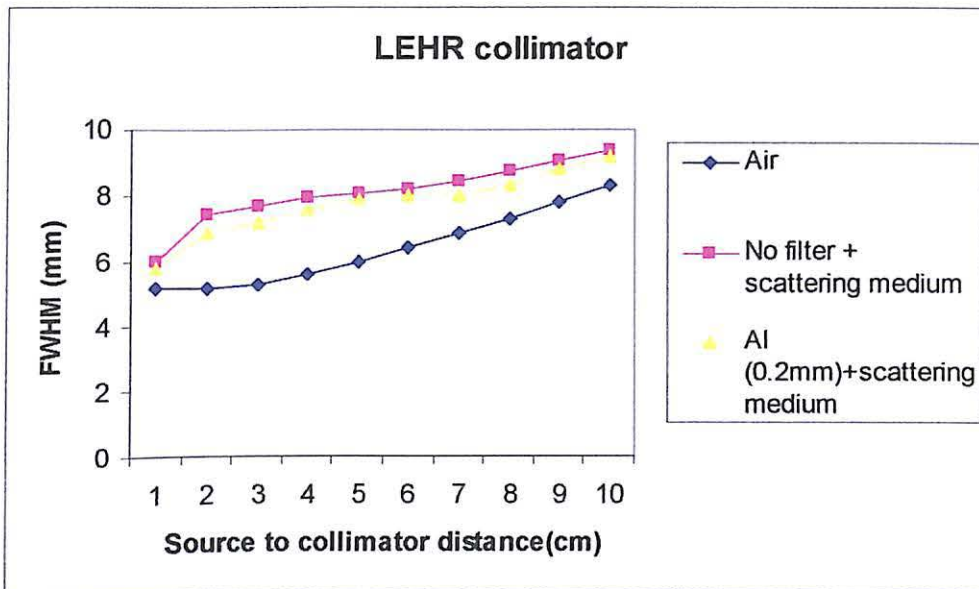
<b>Sensitivity (cps/mCi)</b>	
<b>No Filter</b>	6948.01
<b>Al 0.2mm</b>	6865.78
<b>Al 0.3mm</b>	6821.63

Table 2: The sensitivity without and with material filter for LEGP collimator.

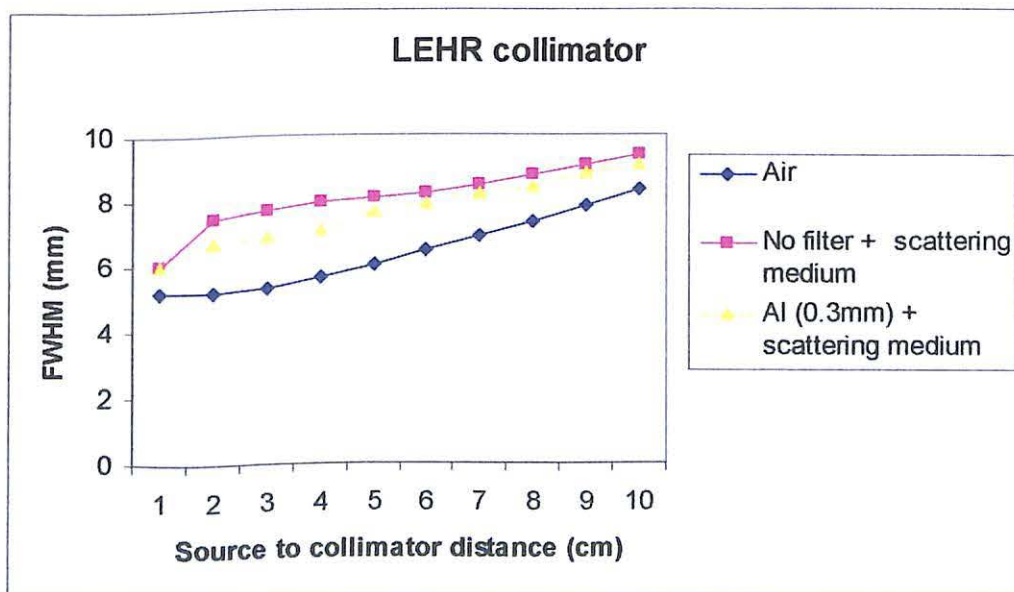
### **System spatial resolution analysis**

Spatial resolution can be defined in terms of the amount by which a system smears out of the image of a thin line source of radioactivity [6]. A profile of the counts measured along a line source is called the line spread function (LSF). To obtain accurate numerical results from the LSF the diameter of line source must be less than or equal to  $\frac{1}{4}$ th FWHM [4]. Resolution can be expressed as the full-width half-maximum (FWHM) of the line spread function measurements.

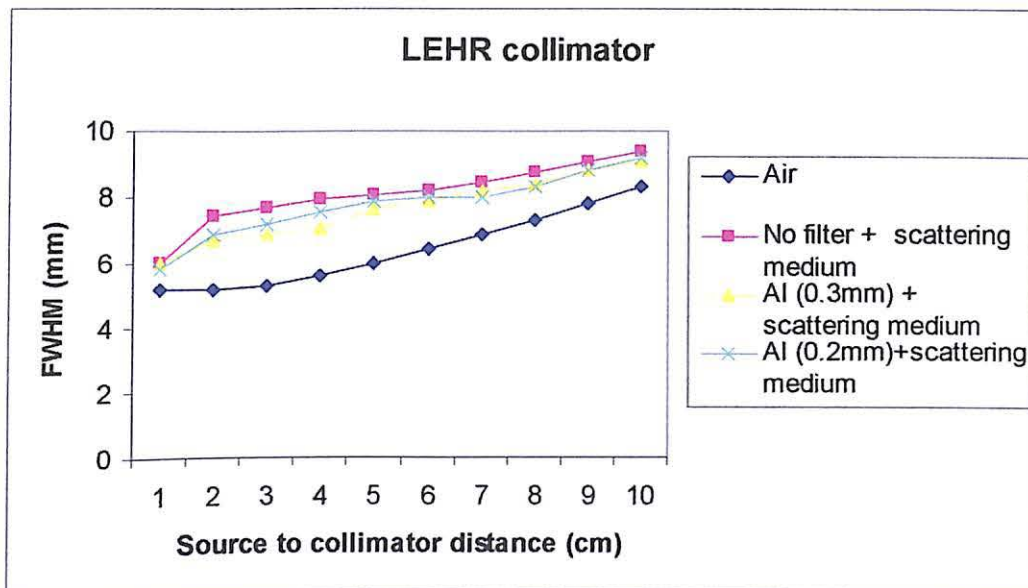
System spatial resolution is defined as the FWHM of a line source measured with the collimator in place. A capillary tube filled with radioactivity was imaged at a fixed distance from the collimator face, and the FWHM was calculated from the image. System spatial resolution is determined chiefly by the collimator [6]. Spatial resolution depends upon many factors, such as type of collimator, source to gamma camera distance and statistical fluctuations in the distribution of light photons among the PM tubes. The results presented in graph (1-12) in FWHM and FWTM.



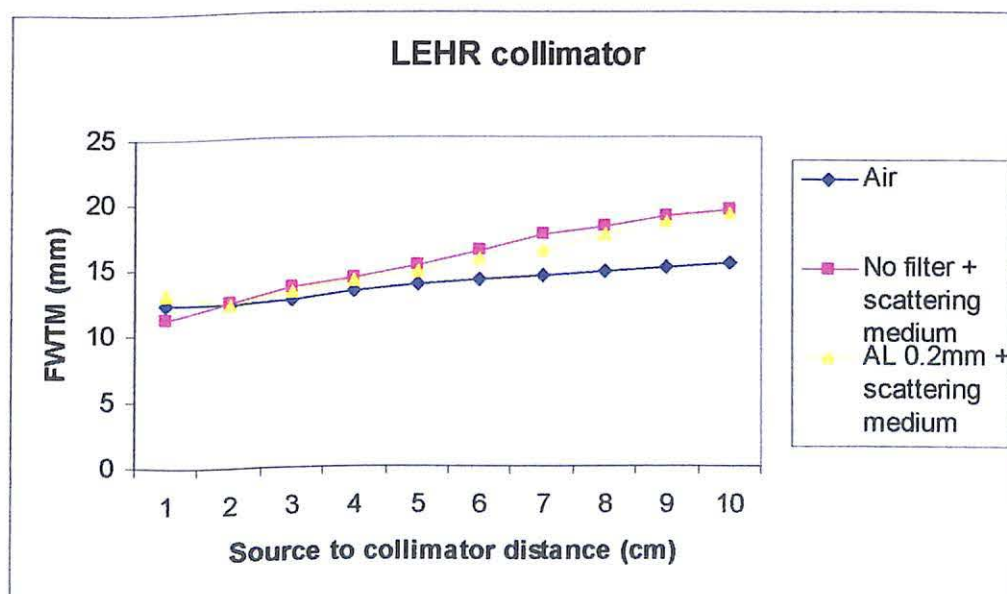
Graph 1: The FWHM values in air and scattering medium without and with aluminum 0.2 mm filter with LEHR collimator.



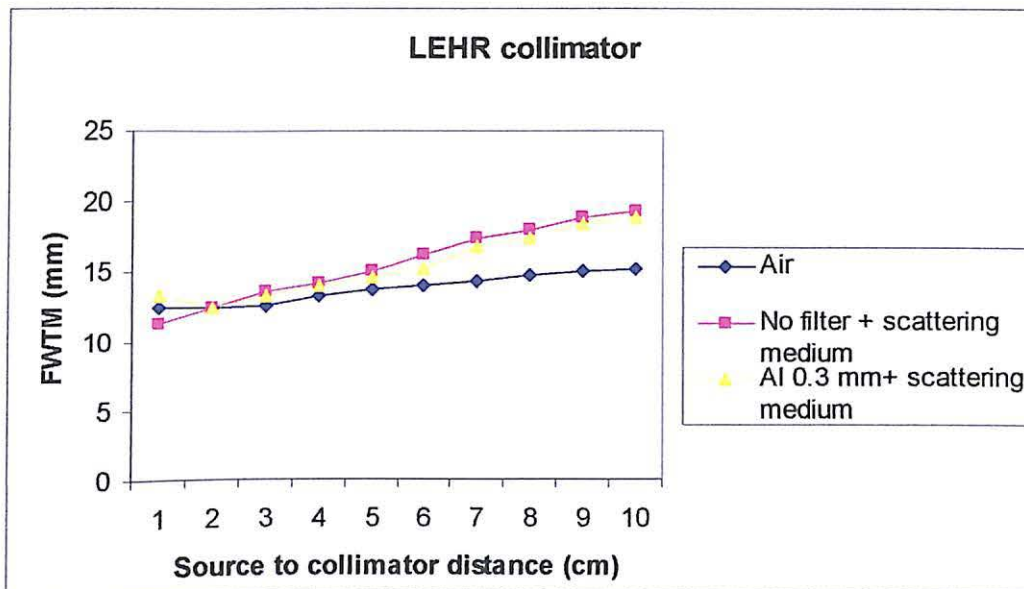
Graph 2: The FWHM values in air and scattering medium without and with aluminum 0.3 mm filter with LEHR collimator.



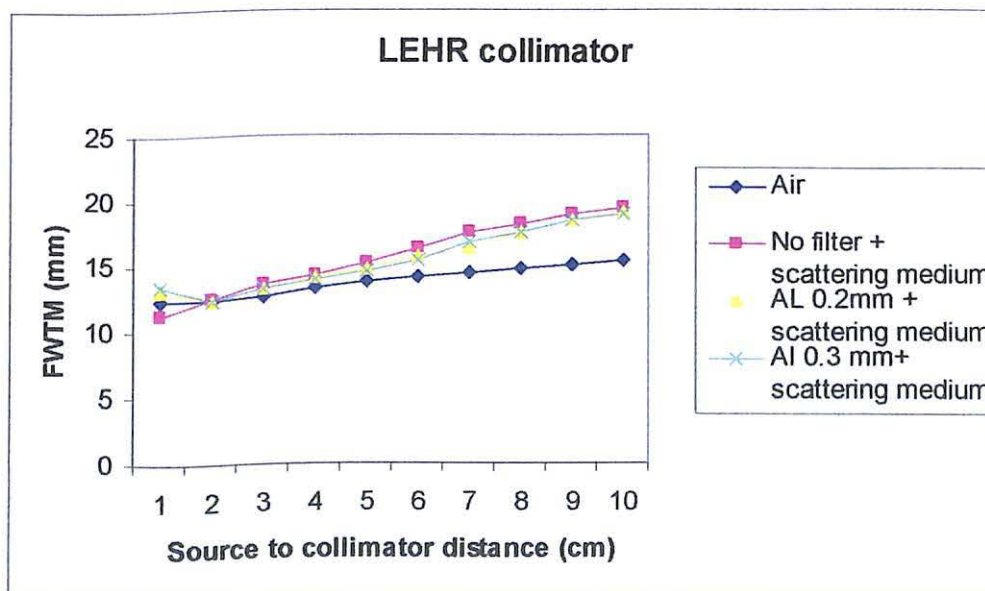
Graph 3: The FWHM values in air and scattering medium without and with aluminum 0.2 and aluminum 0.3 mm filters with LEHR collimator.



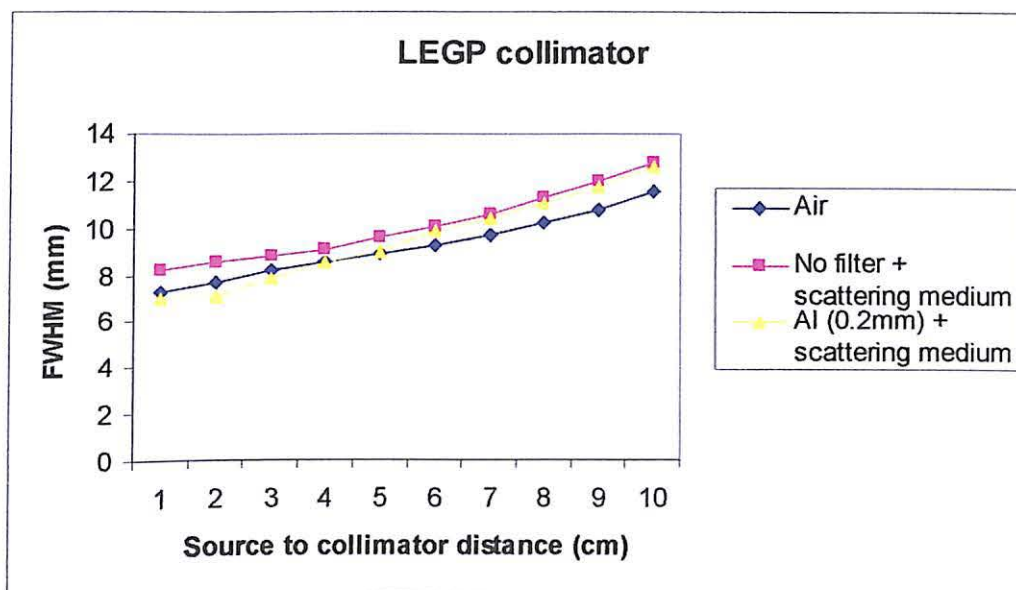
Graph 4: The FWTM values in air and scattering medium without and with aluminum 0.2 mm filter with LEHR collimator.



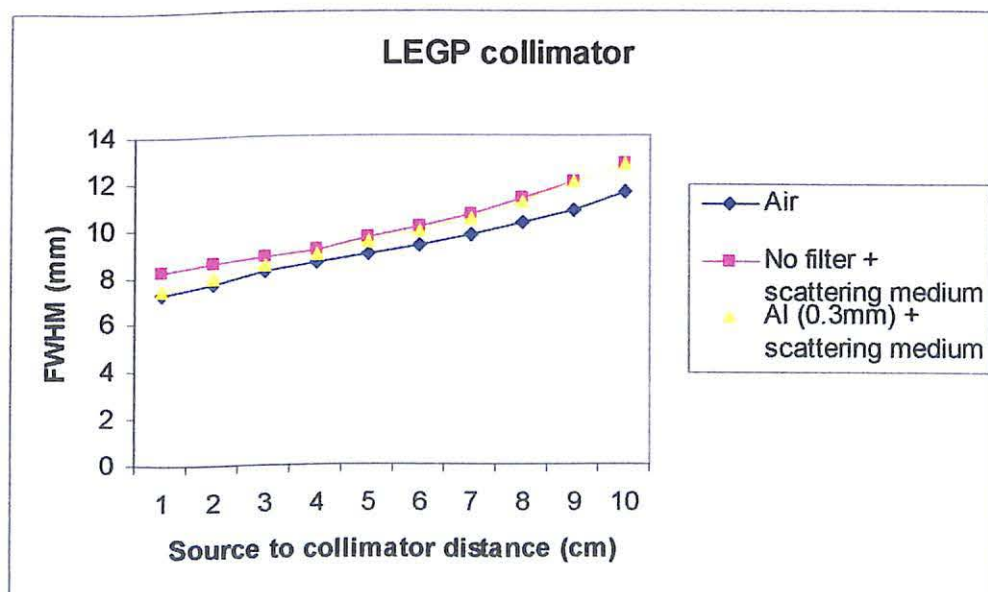
Graph 5: The FWTM values in air and scattering medium without and with aluminum 0.3 mm filter with LEHR collimator.



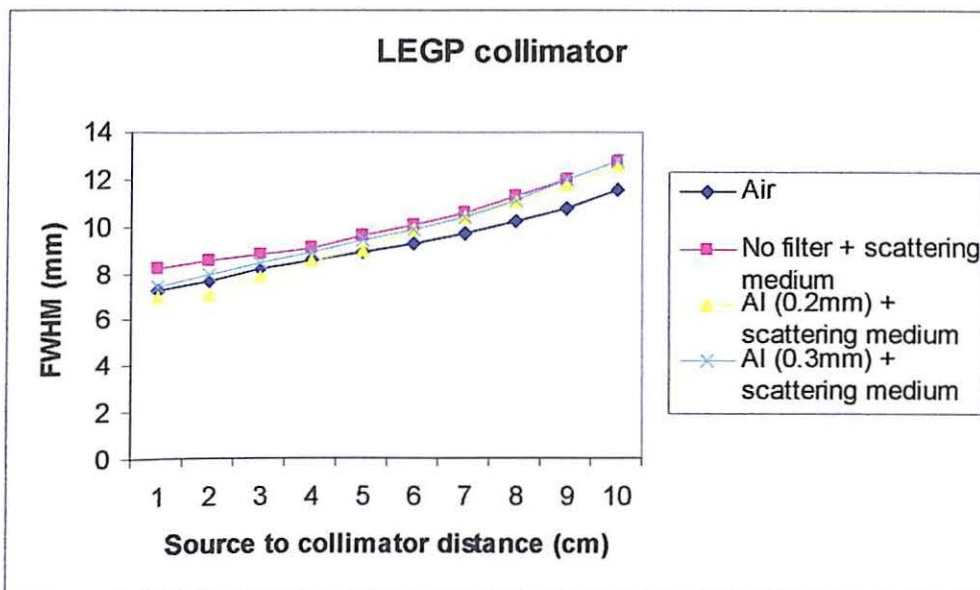
Graph 6: The FWTM values in air and scattering medium without and with aluminum 0.2 mm and aluminum 0.3 mm filters with LEHR collimator.



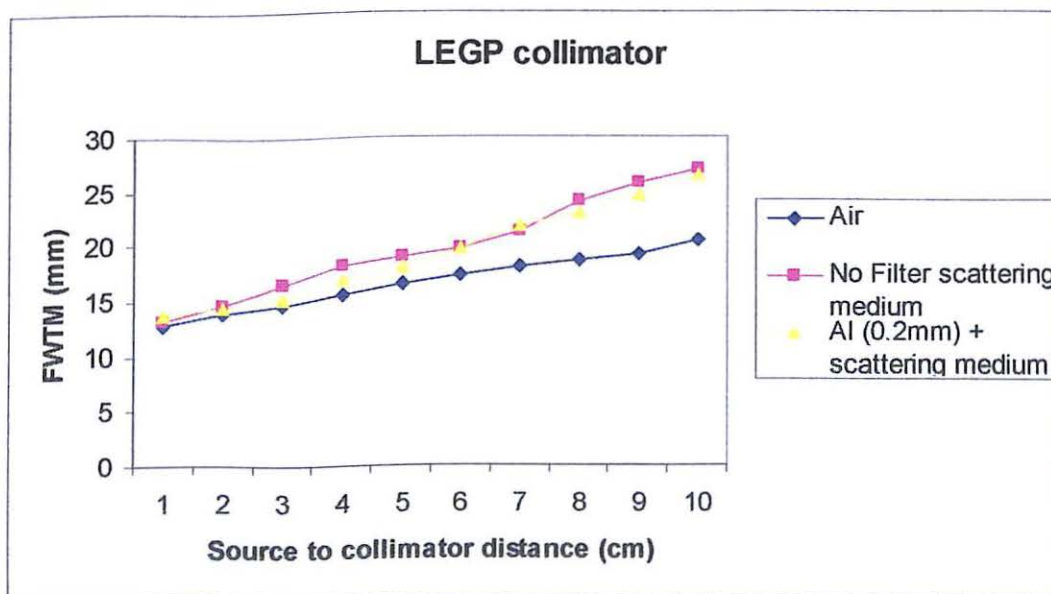
Graph 7: The FWHM values in air and scattering medium without and with aluminum 0.2 mm filter with LEGP collimator.



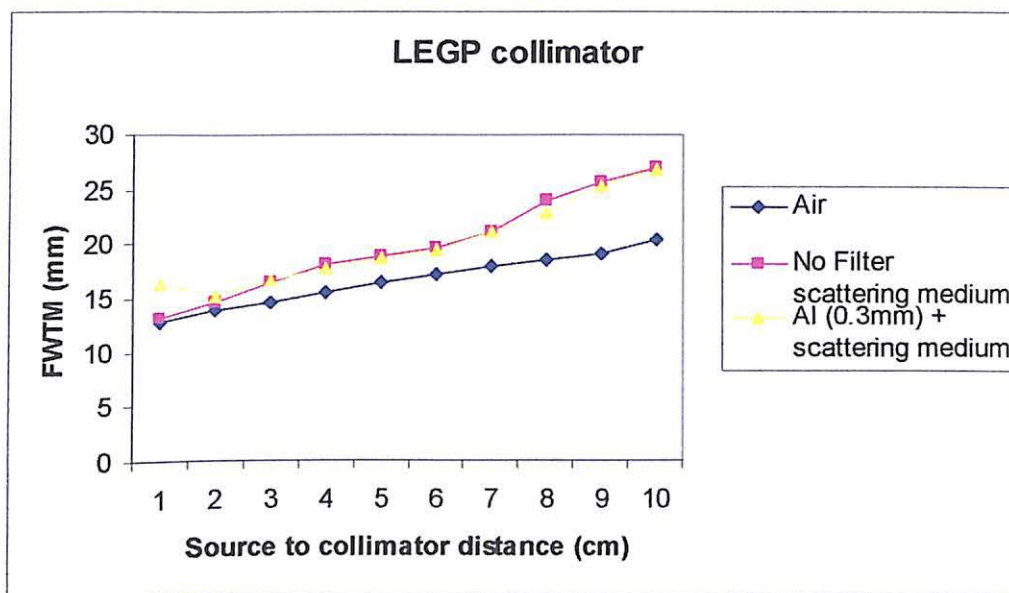
Graph 8: The FWHM values in air and scattering medium without and with aluminum 0.3 mm filter with LEGP collimator.



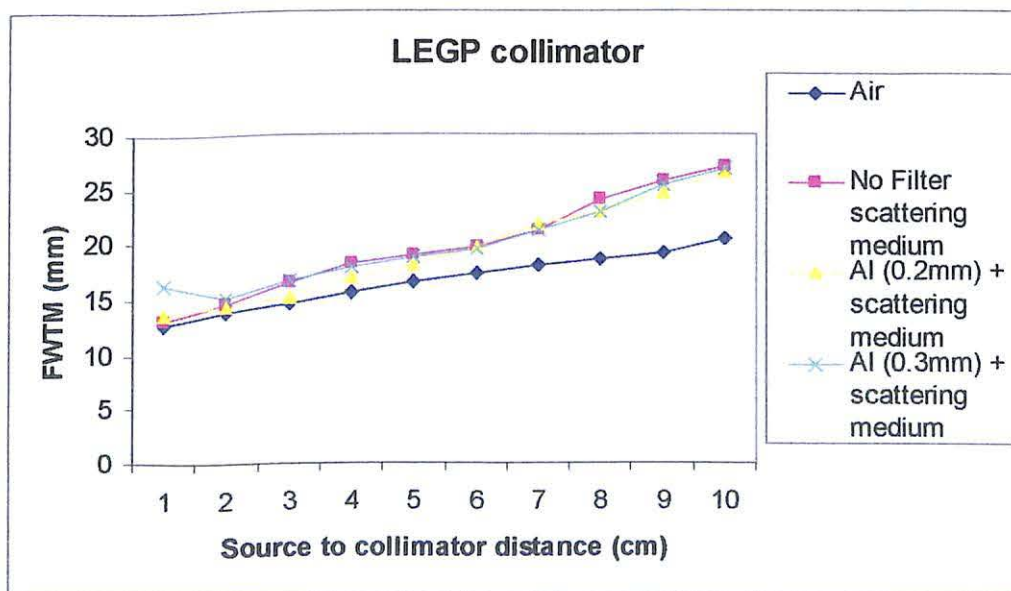
Graph 9: The FWHM values in air and scattering medium without and with aluminum 0.2 mm and aluminum 0.3 mm filters with LEGP collimator.



Graph 10: The FWTM values in air and scattering medium without and with aluminum 0.2 mm filter with LEGP collimator.



Graph 11: The FWTM values in air and scattering medium without and with aluminum 0.3 mm filter with LEGP collimator.



Graph 12: The FWTM values in air and scattering medium without and with aluminum 0.2 mm and aluminum 0.3 mm with LEGP collimator.

## Field uniformity analysis

A key measure of camera performance is the uniformity of response to a flood of activity. This is measured by imaging a uniform flood source of photons, acquiring a large, statistically valid number of counts (>10 000 per pixel) [6]. Flood-field uniformity can be quantified in terms of the difference between the maximum and minimum counts obtained in any pixel divided by the average pixel counts. This approach can give misleading results if there is a single bad value in an otherwise highly uniform field. Probably the best test of uniformity is visual inspection of the images of a flood source [6].

Uniformity was shown by value of useful field of view (UFOV) and central field of view (CFOV). The UFOV is a circular area with a diameter that is the largest inscribed circle within the collimated field of view whereas the CFOV is a circular area with a diameter that is 75 percent of the diameter of the UFOV [8]. The CFOV is centered on the center of the UFOV [8]. Besides, the value of UFOV and CFOV are divided into two measurements which are integral uniformity and differential uniformity. For points within the area of interest (UFOV or CFOV) the maximum and the minimum values are subtracted. This 'span' is divided by the sum of the values at these two points, multiplied by 100, and expressed as a plus or minus percentage integral uniformity. The formula for integral uniformity shall be as follows:

$$\text{Integral uniformity} = \pm 100 [( \max - \min ) / ( \max + \min )] \quad [8]$$

Differential uniformity is a measurement of the worst case rate of change of the flood field over a limited distance. The flood is treated as a number of rows and columns. The numbers of slices for the UFOV in both X and Y direction are approximately 2 x 60 x 0.95

and for the CFOV is approximately 2 x 60 x 0.75. Each slice is processed by starting at one end, examining for 5 pixels from the start pixel and recording the maximum difference. For each slice, a largest deviation is found and for the whole set of slices (for the UFOV or CFOV), a largest deviation is divided by the sum of the values for the two points representing the largest deviation, multiplied by 100 and expressed as a plus or minus percentage differential uniformity for the CFOV and UFOV.

$$\text{Differential uniformity} = \pm \{ [\text{largest slice deviation}(\text{max-min})/[\text{max} + \text{min}]] \} \quad [8]$$

Low energy high resolution

CONDITION	UFOV		CFOV	
	Integral Uniformity (%)	Differential Uniformity (%)	Integral Uniformity (%)	Differential Uniformity (%)
NO FILTER	8.8	(x) :3.0 (y) :3.8	6.8	(x) :3.0 (y) :2.6
ALUMINIUM ( 0.2mm)	8.5	(x) :3.0 (y) :3.7	6.4	(x) :3.0 (y) :2.3
ALUMINIUM (0.3mm)	8.5	(x) :3.0 (y) :3.5	6.7	(x) :3.3 (y) :2.7

Table 3: The UFOV and CFOV uniformity shown in integral and differential uniformity without and with material filters with LEHR collimator.

Low energy general purpose

CONDITION	UFOV		CFOV	
	Integral Uniformity ( % )	Differential Uniformity ( % )	Integral Uniformity ( % )	Differential Uniformity ( % )
NO FILTER	8.8	(x) :3.3 (y) :4.0	6.9	(x) :3.3 (y) :2.9
ALUMINIUM ( 0.2mm)	8.8	(x) :3.5 (y) :4.0	6.5	(x) :3.5 (y) :2.9
ALUMINIUM (0.3mm)	8.6	(x) :3.2 (y) :3.9	7.0	(x) :3.2 (y) :2.6

Table 4: The UFOV and CFOV uniformity shown in integral and differential uniformity without and with material filters with LEGP collimator.

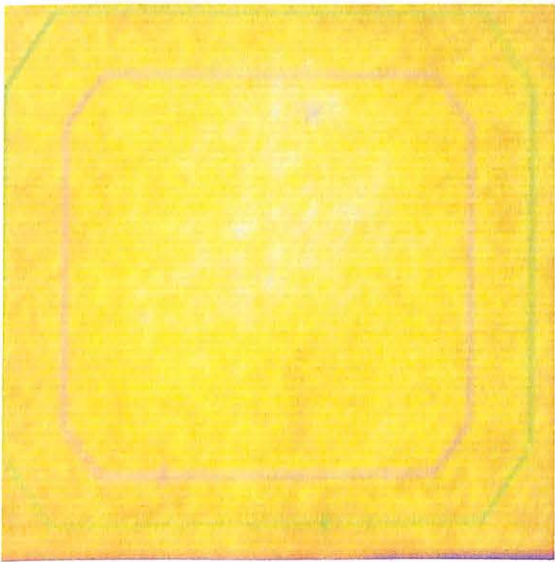


Figure 10: The uniformity without material filter with LEHR collimator